Int. Journal of Refractory Metals and Hard Materials 33 (2012) 75–86

Contents lists available at SciVerse ScienceDirect

Int. Journal of Refractory Metals and Hard Materials

journal homepage: www.elsevier.com/locate/IJRMHM

Machinability investigations on hardened AISI 4340 steel using coated carbide insert

R. Suresh [a], S. Basavarajappa [b], V.N. Gaitonde [c,*], G.L. Samuel [d]

[a] Department of Mechanical Engineering, Canara Engineering College, Mangalore-574 219, Karnataka, India
[b] Department of Mechanical Engineering, University B D T College of Engineering, Davangere-577 004, Karnataka, India
[c] Department of Industrial and Production Engineering, B. V. B. College of Engineering and Technology, Hubli-580 031, Karnataka, India
[d] Department of Mechanical Engineering, Indian Institute Technology Madras, Chennai-600 036, Tamil Nadu, India

ARTICLE INFO

Article history:
Received 13 October 2011
Accepted 24 February 2012

Keywords:
Hard turning
AISI 4340 high strength low alloy steel
Coated carbide inserts
Machinability
Design of experiments
Response surface methodology

ABSTRACT

The hard turning process with advanced cutting tool materials has several advantages over grinding such as short cycle time, process flexibility, compatible surface roughness, higher material removal rate and less environment problems without the use of cutting fluid. However, the main concerns of hard turning are the cost of expensive tool materials and the effect of the process on machinability characteristics. The poor selection of the process parameters may cause excessive tool wear and increased work surface roughness. Hence, there is a need to study the machinability aspects in high-hardened components. In this work, an attempt has been made to analyze the influence of cutting speed, feed rate, depth of cut and machining time on machinability characteristics such as machining force, surface roughness and tool wear using response surface methodology (RSM) based second order mathematical models during turning of AISI 4340 high strength low alloy steel using coated carbide inserts. The experiments were planned as per full factorial design (FFD). From the parametric analysis, it is revealed that, the combination of low feed rate, low depth of cut and low machining time with high cutting speed is beneficial for minimizing the machining force and surface roughness. On the other hand, the interaction plots suggest that employing lower cutting speed with lower feed rate can reduce tool wear. Chip morphology study indicates the formation of various types of chips operating under several cutting conditions.

1. Introduction

The machining of hardened steel components (45–65 HRC); an alternative to conventional grinding process is a cost-effective and flexible machining process for ferrous metal components and hence broadly used in many applications such as tools, dies and molds, gears, cams, shafts, axles, bearings and forgings [1–4]. The machining of hard steel using advanced tool materials like coated carbide, mixed ceramic and cubic boron nitride has more advantages than grinding or polishing such as shorter lead times, reduced processing costs, improved material properties, compatible surface roughness, higher material removal rate, ability to machine thin wall sections and less environment problems without the use of cutting fluid. It has also been reported that the resulting machining time reduction is as high as 60% in hard turning [5]. This process has become a normal practice in industry because of increased productivity and reduced energy consumption [6–8].

The hard turning can offer a reasonably high accuracy for the hardened components, but the major problems occur with surface quality and tool wear [9,10]. The formation of tempered white and dark layers in machined surfaces and the generation of undesirable residual stresses significantly affect the product quality of hardened component [11,12]. Moreover, the cutting tools used for hard turning are relatively costly as compared to grinding and hence there is a need to investigate the effect of machining parameters on tool life. It has also been reported that the properties and the composition of tool materials are critical to the behavior of machining forces, which in turn affect the surface finish and tool life [13]. Therefore, it is necessary to study the influence of process parameters on machinability characteristics, particularly on machining force, surface roughness and tool wear in hard turning process.

Advances in coating technology have resulted in a new generation of high performance coated carbide tools, which exhibit improved properties such as fracture strength, toughness, thermal shock resistance, wear resistance and hardness. The surfaces of cemented carbide cutting tools need to be abrasion resistant, hard and chemically inert to prevent the tool and the work material from interacting chemically with each other during machining. The coated carbides are basically cemented carbide insert material coated with one or more thin layers of wear resistant, such as titanium carbide (TiC), titanium nitride (TiN) and/or aluminum oxide (Al_2O_3) [14]. It has been

* Corresponding author. Tel.: +91 836 2378275; fax: +91 836 2374985.
E-mail addresses: sureshchiru09@gmail.com (R. Suresh), basavarajappas@yahoo.com (S. Basavarajappa), gaitondevn@yahoo.co.in (V.N. Gaitonde), samuelgl@iitm.ac.in (G.L. Samuel).

0263-4368/$ – see front matter © 2012 Elsevier Ltd. All rights reserved.
doi:10.1016/j.ijrmhm.2012.02.019

reported that thin (0.1 to 30 μm) hard (>2500VHN) coatings can reduce tool wear and improve tool life as well as productivity [15].

Several investigations have been carried out to study the performance of coated carbide, ceramic and cubic boron nitride (CBN) tools during machining of hard materials. Luo et al. [16] studied wear behavior in turning of AISI 4340 hardened alloy steels using CBN and ceramic tools. It was reported that the main wear mechanism for CBN tool was abrasion, whereas the adhesion and abrasion were dominant for ceramic tools. Additionally, tool life was increased with the cutting speed for both cutting tools due to the formation of a protective layer on the tool–chip interface. An increase in workpiece hardness leads to lower wear rates. Yallase et al. [17] experimentally investigated the behavior of CBN tools during hard turning of AISI 52100-tempered steel. The surface quality obtained with the CBN tool was found to be significantly better than grinding. A relationship between flank wear and surface roughness was also established based on an extensive experimental data.

Davim and Figueira [18] performed experimental investigations on AISI D2 cold work tool steel (60 HRC) using ceramic tools composed approximately of 70% Al_2O_3 and 30% TiC in surface finish operations. A combined technique using an orthogonal array (OA) and analysis of variance (ANOVA) was employed in their study. The test results showed that it was possible to achieve surface roughness levels as low as R_a<0.8 mm with an appropriate choice of cutting parameters that eliminated cylindrical grinding. Lima et al. [15] evaluated the machinability of hardened AISI 4340 and D2 grade steels at different levels of hardness by using various cutting tool materials. The AISI 4340 steels were hardened to 42 and 48 HRC and then turned by using coated carbide and CBN inserts. The higher cutting forces were recorded when AISI 4340 steel was turned using low feed rates and depth of cut and lower surface roughness values were observed for softer workpiece materials as cutting speed was elevated and they deteriorated with feed rate. Ozel and Karpat [19] used regression and artificial neural network models for predicting the surface roughness and tool wear in hard turning of AISI H13 steel using CBN inserts. Quiza et al. [20] applied artificial neural networks (ANN) and multiple regression models for predicting tool wear in hard machining of AISI D2 steel using ceramic inserts. They found that the neural network model could predict tool wear accurately compared to regression model. Tamizharasan et al. [21] analyzed the tool life, tool wear, material removal rate and economy of hard turning of hardened petrol engine crank pin material by using three grades of CBN tools.

Oliviera et al. [22] investigated the hard turning of AISI 4340 steel (56 HRC) in continuous and interrupted cuts with PCBN and whisker-reinforced cutting tools. The results indicated that the longest tool life could be achieved in continuous turning by PCBN tool. On the other hand, similar tool life values were obtained during interrupted turning using both the PCBN and ceramic tools. However, PCBN showed better results in terms of surface roughness. Jiang et al. [23] addressed the surface morphology, surface roughness, coating cross-section, chemical composition, crystal structure, micro hardness, adhesion and wear life issues of CBN-based coating deposition on carbide inserts (SNMG 120408) for finish hard turning of hardened AISI 4340 steel. The surface quality of machined work pieces in terms of surface roughness and white layer formation was also analyzed. Aslan [24] described the performance and wear behavior of TiN-coated tungsten carbide, TiCN/TiAlN coated tungsten carbide, TiAlN coated cermet, a mixed ceramic of Al_2O_3/TiCN and CBN tools in high-speed cutting of AISI D3 cold work tool steel (62 HRC). The CBN tool exhibited the best cutting performance in terms of both flank wear and surface finish. In addition, the highest volume of material removal was obtained with CBN tool.

An investigative study by Yigit et al. [25] indicated that a multilayer TiCN/TiC/Al_2O_3/TiN coating (10.5 μm thick) with an external TiN layer was the best-suited tool for minimizing flank wear and surface roughness in hard turning. Aneiro et al. [26] have studied performance of TiCN/Al_2O_3/TiN coated carbide and PCBN tools during turning of hardened steel. They observed that better tool life could be achieved using PCBN tools, but the cost of PCBN tool is as twice as that of the coated carbide tool. The machining medium hardened steels with TiCN/Al_2O_3/TiN inserts tend to be more productive. The relatively good performance of coated carbide tools on machining hardened steel relied on coating combination of layers, which seems to be the adequate one for such applications. Knutsson et al. [27] demonstrated that improved wear resistance of TiAlN/TiN multilayer attributed to the multilayer hardening effects and improved thermal stability during hard turning.

Yigit et al. [28] found that multilayer coating on carbide substrate enhances the tool life performance and cutting force decreases using high temperature chemical vapor deposition (HTCVD) multilayer carbide tools when compared to uncoated carbide tools. Ciftci [29] investigated the dry turning of austenitic stainless steels using CVD multilayer-coated cemented carbide tools. It was reported that TiN coating has a lower coefficient of friction than Al_2O_3 coating. Bouzoukis et al. [30] stated that the film failure development after the coating fracture initiation was less intense in case of multilayer coating and can be attributed to the deceleration of potential cracks propagation within the layered TiN/TiAlN structure. They reported that by applying the multilayer coatings tool life could be improved.

Grzesik [31] described the characterization of surface roughness generated during hard turning operations of AISI 5140 (60 HRC) steels with conventional and wiper ceramic tools at variable feed rate conditions. Gaitonde et al. [32] explored the effects of depth of cut and machining time on machinability aspects such as machining force, power, specific cutting force, surface roughness, and tool wear by using second-order mathematical models during turning of high chromium content AISI D2 cold work tool steel with CC650, CC650WG and GC6050WH ceramic inserts. Their results revealed that CC650WG wiper insert performed better with respect to surface roughness and tool wear, whereas the CC650 conventional insert was useful in reducing the machining force, power, and specific cutting force. The influence of cutting speed, feed rate and machining time on machinability aspects such as specific cutting force, surface roughness and tool wear in AISI D2 cold work tool steel hard turning was studied by Gaitonde et al. using RSM [33] and ANN [34] based models.

Arsecularatne et al. [35] performed an experimental investigation on machining of AISI D2 steel (62 HRC) with PCBN tools. The most feasible feed rate was found to be in the range 0.08–0.20 mm/rev and speed in the range 70–120 m/min. Kumar et al. [36] conducted machining studies on hardened martensitic stainless steel (60 HRC) to demonstrate the effect of tool wear on tool life of alumina ceramic cutting tools. The multiple regression models of flank wear, crater wear and notch wear were developed to predict the tool wear mechanisms. More et al. [37] experimentally investigated the effects of cutting speed and feed rate on tool wear, surface roughness and cutting forces in turning of AISI 4340 hardened steel using CBN–TiN-coated carbide inserts. In addition, cost analysis based on total machining cost per part was also performed for the economic comparison of CBN–TiN-coated and PCBN inserts.

Chou et al. [38,39], Thiele et al. [13,40] and Ozel et al. [41] explained the effects of various factors affecting cutting forces, surface roughness, tool wear and surface integrity in hard turning of various grades of steels using CBN tools. Poulachon et al. [42] analyzed the tool wear behavior by considering the effect of microstructure of hardened steels. El-Wardany et al. [43,44] in their study reported the effects of cutting parameters and tool wear on chip morphology, quality and integrity of machined surfaces during high speed turning of AISI D2 work tool steel. Kishawy and Elbestawi [45] illustrated the tool wear mechanism and surface integrity during hard-speed turning of AISI D2 cold work tool steel. Chou and song [46] concluded that better surface finish could be achieved using a large tool nose radius on finish turning of AISI 52100 bearing steel using alumina titanium-carbide tools but generates deeper white layers.

Benga and Abrao [47] and Kumar et al. [48] observed superior surface quality in turning of hardened steel components using alumina-TiC ceramic tools. Grzesik and Wanat [49,50] and Klocke and Kratz [51] presented 2D and 3D analysis of surface finish in hard turning. Grzesik [31] assessed the surface roughness characteristics during hard turning operations with conventional and wiper ceramic cutting tools at variable feed rates. Schwach and Guo [52] investigated the surface topography, surface roughness, micro-hardness, subsurface microstructure and residual stresses of turned AISI 52100 components. Pavel et al. [53] focused mainly on the effect of tool wear on surface finish in interrupted and continuous hard turning. Diniz and Oliveira [54] identified economical tool material and tool cutting edge micro geometry for optimizing tool wear and tool life in continuous, semi interrupted and interrupted cutting of AISI 4340 hardened steel.

According to Ezugwu et al. [55], PCBN tools offer excellent performance during machining hardened steels; however, their costs are relatively higher as compared to carbide tools. The present work assesses some aspects of turning of hardened AISI 4340 (48 HRC) steel with multilayer CVD coated (TiN/MT TiCN/Al_2O_3) carbide tool. An attempt has been in this paper to analyze the effects of cutting speed, feed rate, depth of cut and machining time during hard turning on various aspects of machinability such as machining force, surface roughness and tool wear by developing second order mathematical models based on response surface methodology (RSM). The RSM based mathematical modeling using design of experiments (DOE) is proved to be an efficient modeling tool [56]. The RSM not only reduces the cost and time but also gives the necessary information about the main and interaction effects of process parameters.

2. Response surface methodology

The response surface methodology (RSM) is a modeling tool used for establishing the relationship(s) between the independent variables and the desired response(s) and searching the importance of these variables on various performance criteria. The RSM is useful for developing, analyzing, improving and optimizing the product/process that provides an overall perspective of the system response within the design space [56]. The modeling of desired response to various process variables can be obtained through design of experiments (DOE) and applying the regression technique. The DOE provides an occasion to study the individual as well as interaction effects of process variables with the minimum number of experiments that can significantly reduce the experiments as compared to traditional experimental design. The RSM adopts mathematical and statistical techniques to demonstrate the influence of interactions of process variables on desired responses when they are varied simultaneously.

In several situations, it is possible to represent the independent process parameters in quantitative form and the response in terms of process parameters can be expressed as [56]:

$$Y = \phi(x_1, x_2, x_3, \ldots\ldots x_k) \quad (1)$$

where Y is the response, $x_1, x_2, x_3, \ldots\ldots x_k$ are the quantitative factors and ϕ is the response function. It can be approximated within the experimental region by a polynomial when the mathematical form of response function is unknown. Higher the degree of polynomial better the correlation but the experimentation costs will increase.

3. Experimental details

3.1. Planning of experiments

The planning of experiments is vital to develop the mathematical models based on RSM. The mathematical modeling provides reliable equations obtained from the data of properly designed experiments. In the present investigation, cutting speed (v), feed rate (f), depth of cut (d) and machining time (t) are identified as the process parameters, which affect the various machinability aspects, which is evaluated by three characteristics, namely, machining force (F_m) in operation, surface roughness (R_a) in workpiece and wear (W) on cutting tool. In the current research, the ranges of the process parameters were selected based on authors' preliminary experiments. Four levels for cutting speed, three levels for each of the three parameters, namely feed rate, depth of cut and machining time were selected. The effects of process parameters on machinability are tested through a set of planned experiments based on full factorial design (FFD) to explore the quadratic response surface [56]. Thus 108 trials based on FFD were planned [56]. The machining parameters and their levels are summarized in Table 1 and the experimental layout plan as per FFD for the current investigation is illustrated in Table 2.

3.2. Material, experimentation and machinability assessment

AISI 4340 high strength low alloy steel was used as work material for the current investigation. This work material was chosen based on its application in automobile and machine tool parts such as axle shafts, main shafts, spindles, gears, power transmission gears and couplings. For machining tests, AISI 4340 steel of 100 mm diameter and 400 mm length of 10 pieces were selected from a single bar (L/D ratio is 1:4) and were then used as work piece materials after being heat treated (hardening and tempering) to a hardness of 48 HRC. The chemical composition of AISI 4340 steel was evaluated using an optical emission spectrometer (Baird-DV6E) and is given in Table 3.

The coated carbide inserts of ISO geometry '*CNMG 120408*' with chip breaker were used throughout the investigation. The inserts have a multilayer CVD coating (TiN/MT-TiCN/Al_2O_3) on cemented carbide substrate. The CVD coating consists of a thick, moderate temperature chemical vapor deposition (MT CVD) of TiN for heat resistance and with low coefficient of friction, TiCN for wear resistance and thermally stable and Al_2O_3 for heat and crater wear resistance. The combined top coating and gradient substrate provide extremely good behavior during dry machining. The '*PCLNL2525 M12*' (ISO) type tool holder was used with tool geometry as follows: including angle = 80^0, back rake angle = −6°, clearance angle = 5°, approach angle = 95° and nose radius = 0.8 mm.

The dry turning experiments were performed on hardened AISI 4340 steel material using coated carbide inserts. '*WIDIA CNC*' lathe was employed to conduct the experiments. The lathe is equipped with 22 kW spindle power and a maximum spindle speed of 5000 rpm. Axial and radial run out was checked on the machine, which was found to be within the acceptable limit of error.

During the turning tests, the cutting force (F_c), feed force (F_f) and radial force (F_r) were measured using '*Kistler type 9263A*' three-component piezo-electric dynamometer, which was connected to charged amplifiers and personal computer through an analog to digital converter card. To obtain and record the force data '*WINDUCOM V-3*' data acquisition software was used. Before conducting the experiments, the lathe tool dynamometer was calibrated for data accuracy. A standard load of 50 N was attached with an anchor to the tool dynamometer and the forces were measured. Then the force data were compared with the standard weight. The result of this pre test found that the tool

Table 1
Machining parameters and their selected levels.

Parameter	Level			
	1	2	3	4
Cutting speed (v), m/min	80	140	200	260
Feed rate (f), mm/rev	0.10	0.18	0.26	–
Depth of cut (d), mm	0.8	1.0	1.2	–
Machining time (t), min	2	4	6	–

Table 2
Experimental layout plan as per FFD and the corresponding values of machinability characteristics.

Trial no.	Actual setting values of input parameters				Machinability characteristics		
	v (m/min)	f (mm/rev)	d (mm)	t (min)	F_m (N)	R_a (μm)	W (mm)
1	80	0.10	0.8	2	525.01	0.80	0.050
2	80	0.10	0.8	4	537.17	0.85	0.066
3	80	0.10	0.8	6	556.36	0.91	0.078
4	80	0.18	0.8	2	650.63	1.50	0.060
5	80	0.18	0.8	4	668.99	1.56	0.072
6	80	0.18	0.8	6	693.73	1.64	0.084
7	80	0.26	0.8	2	782.79	2.30	0.074
8	80	0.26	0.8	4	798.80	2.40	0.088
9	80	0.26	0.8	6	817.94	2.45	0.096
10	140	0.10	0.8	2	451.09	0.65	0.065
11	140	0.10	0.8	4	469.60	0.70	0.082
12	140	0.10	0.8	6	490.94	0.78	0.100
13	140	0.18	0.8	2	622.31	1.30	0.074
14	140	0.18	0.8	4	644.22	1.40	0.096
15	140	0.18	0.8	6	676.29	1.48	0.110
16	140	0.26	0.8	2	744.42	2.10	0.098
17	140	0.26	0.8	4	764.94	2.23	0.112
18	140	0.26	0.8	6	782.68	2.38	0.120
19	200	0.10	0.8	2	412.49	0.56	0.075
20	200	0.10	0.8	4	430.56	0.60	0.088
21	200	0.10	0.8	6	448.72	0.65	0.110
22	200	0.18	0.8	2	605.86	1.00	0.085
23	200	0.18	0.8	4	621.43	1.10	0.100
24	200	0.18	0.8	6	645.03	1.12	0.118
25	200	0.26	0.8	2	707.00	1.80	0.108
26	200	0.26	0.8	4	727.63	1.92	0.118
27	200	0.26	0.8	6	749.21	1.98	0.129
28	260	0.10	0.8	2	408.55	0.50	0.091
29	260	0.10	0.8	4	411.86	0.55	0.106
30	260	0.10	0.8	6	430.94	0.60	0.120
31	260	0.18	0.8	2	568.61	0.85	0.107
32	260	0.18	0.8	4	585.41	0.90	0.115
33	260	0.18	0.8	6	605.77	1.00	0.127
34	260	0.26	0.8	2	676.70	1.74	0.120
35	260	0.26	0.8	4	692.83	1.80	0.128
36	260	0.26	0.8	6	711.18	1.82	0.134
37	80	0.10	1.0	2	609.8	0.90	0.075
38	80	0.10	1.0	4	625.55	0.95	0.085
39	80	0.10	1.0	6	643.71	0.98	0.100
40	80	0.18	1.0	2	794.15	1.20	0.090
41	80	0.18	1.0	4	810.40	1.25	0.105
42	80	0.18	1.0	6	828.66	1.34	0.118
43	80	0.26	1.0	2	925.05	1.80	0.105
44	80	0.26	1.0	4	939.62	1.90	0.120
45	80	0.26	1.0	6	966.18	1.98	0.130
46	140	0.10	1.0	2	549.13	0.85	0.089
47	140	0.10	1.0	4	561.21	0.90	0.100
48	140	0.10	1.0	6	585.49	0.98	0.118
49	140	0.18	1.0	2	752.99	1.04	0.105
50	140	0.18	1.0	4	769.36	1.10	0.120
51	140	0.18	1.0	6	793.03	1.25	0.127
52	140	0.26	1.0	2	891.90	1.60	0.115
53	140	0.26	1.0	4	903.46	1.70	0.128
54	140	0.26	1.0	6	922.43	1.80	0.144
55	200	0.10	1.0	2	531.66	0.65	0.105
56	200	0.10	1.0	4	546.73	0.70	0.120
57	200	0.10	1.0	6	560.64	0.85	0.130
58	200	0.18	1.0	2	703.96	0.95	0.117
59	200	0.18	1.0	4	722.54	1.00	0.128
60	200	0.18	1.0	6	744.76	1.15	0.135
61	200	0.26	1.0	2	835.83	1.20	0.124
62	200	0.26	1.0	4	848.57	1.30	0.140
63	200	0.26	1.0	6	865.71	1.45	0.155
64	260	0.10	1.0	2	489.44	0.50	0.116
65	260	0.10	1.0	4	506.94	0.60	0.130
66	260	0.10	1.0	6	525.22	0.68	0.145
67	260	0.18	1.0	2	659.72	0.70	0.126
68	260	0.18	1.0	4	672.25	0.72	0.139
69	260	0.18	1.0	6	688.39	0.84	0.156
70	260	0.26	1.0	2	797.28	1.00	0.135
71	260	0.26	1.0	4	816.92	1.20	0.155
72	260	0.26	1.0	6	831.69	1.30	0.168
73	80	0.10	1.2	2	651.73	1.00	0.095
74	80	0.10	1.2	4	665.33	1.10	0.107
75	80	0.10	1.2	6	681.18	1.15	0.115
76	80	0.18	1.2	2	874.19	1.30	0.110
77	80	0.18	1.2	4	890.06	1.35	0.125
78	80	0.18	1.2	6	904.90	1.45	0.134
79	80	0.26	1.2	2	1036.08	1.50	0.125
80	80	0.26	1.2	4	1054.65	1.65	0.138
81	80	0.26	1.2	6	1071.29	1.80	0.156
82	140	0.10	1.2	2	614.23	0.84	0.107
83	140	0.10	1.2	4	631.61	0.90	0.114
84	140	0.10	1.2	6	645.63	0.95	0.125
85	140	0.18	1.2	2	826.43	1.16	0.116
86	140	0.18	1.2	4	841.22	1.20	0.129
87	140	0.18	1.2	6	857.59	1.30	0.145
88	140	0.26	1.2	2	1011.83	1.40	0.134
89	140	0.26	1.2	4	1027.12	1.50	0.142
90	140	0.26	1.2	6	1038.20	1.70	0.165
91	200	0.10	1.2	2	598.10	0.90	0.110
92	200	0.10	1.2	4	613.44	0.95	0.125
93	200	0.10	1.2	6	627.55	1.00	0.135
94	200	0.18	1.2	2	788.86	1.04	0.126
95	200	0.18	1.2	4	808.74	1.10	0.138
96	200	0.18	1.2	6	826.58	1.15	0.156
97	200	0.26	1.2	2	990.07	1.25	0.145
98	200	0.26	1.2	4	1006.47	1.30	0.154
99	200	0.26	1.2	6	1019.30	1.50	0.178
100	260	0.10	1.2	2	581.52	0.80	0.125
101	260	0.10	1.2	4	593.45	0.90	0.132
102	260	0.10	1.2	6	606.38	0.95	0.152
103	260	0.18	1.2	2	757.83	0.90	0.134
104	260	0.18	1.2	4	778.58	1.00	0.146
105	260	0.18	1.2	6	798.30	1.05	0.168
106	260	0.26	1.2	2	959.53	1.04	0.158
107	260	0.26	1.2	4	975.28	1.20	0.176
108	260	0.26	1.2	6	997.93	1.30	0.194

dynamometer had errors, but within the acceptable limit. The machining test was conducted with a fresh cutting edge for cutting time of 2, 4 and 6 min. The machining force (F_m) is determined from the following equation:

$$F_m = \sqrt{F_c^2 + F_f^2 + F_r^2} \tag{2}$$

After the trials the tools were cleaned in an HCl solution and acetone in order to remove steel residuals adhered to the rake and flank face of the cutting tools. The width of flank wear was (W) measured using a '*Nikon*' optical microscope connected to a digital camera and computer. The surface roughness values were measured immediately after the turning process at five different locations on work piece by using '*Mitutoyo® Surftest-201*' surface roughness tester. The average of five roughness values was taken as an arithmetic surface roughness (R_a).

The computed values of machining force (F_m), and measured values of surface roughness (R_a) and tool wear (W) are presented in Table 2. The photographs of the experimental setup with measurement of the cutting forces by piezoelectric dynamometer and the charge amplifiers with PC based data acquisition system are shown in Fig. 1.

Table 3
Chemical composition of AISI 4340 work material (wt.%).

C	Si	Mn	P	S	Cr	Ni	Mo	Fe
0.382	0.228	0.609	0.026	0.022	0.995	1.514	0.226	95.998

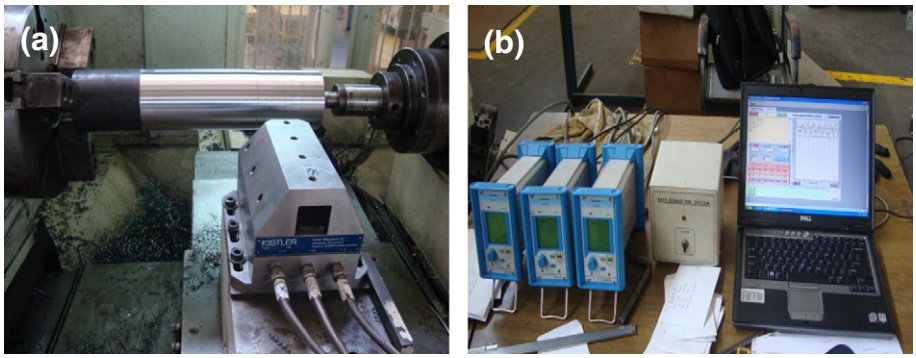

Fig. 1. (a) Experimental setup with measurement of cutting forces by piezoelectric dynamometer. (b) Charge amplifiers and PC based data acquisition system.

4. Development of machinability models

In the present investigation, the RSM based mathematical models for machining force (F_m), surface roughness (R_a) and tool wear (W) have been developed with cutting speed (v), feed rate (f), depth of cut (d) and machining time (t) as the process parameters. The response surface equation considering two factor interactions is given by [56]:

$$Y = b_0 + b_1 v + b_2 f + b_3 d + b_4 t + b_{11} v^2 + b_{22} f^2 + b_{33} d^2 + b_{44} t^2 + b_{12} vf + b_{13} vd + b_{14} vt + b_{23} fd + b_{24} ft + b_{34} dt \quad (3)$$

where, Y is the desired response and b_o, b_1,... b_{34}: regression coefficients of polynomial equation to be determined for each response. The regression coefficients of linear, quadratic and interaction terms of mathematical models are determined by [56]:

$$b = \left(X^T X\right)^{-1} X^T Y \quad (4)$$

where, b is the matrix of process parameter estimates; X is the calculation matrix, which includes linear, quadratic and interaction terms; X^T is the transpose of X and Y is the matrix of desired response. The mathematical models as determined by multiple regression analysis [56] to predict the machining force (F_m), surface roughness (R_a) and tool wear (W) during hard turning of AISI 4340 steel using coated carbide insert are given by [56]:

$$F_m = -69.5277 - 1.057749v + 1510.257f + 656.4995d + 9.20767535t + 0.000709002v^2 - 3159.87413f^2 - 233.288194d^2 + 0.34868056t^2 - 0.095729167vf + 0.2595787vd - 0.003147222vt + 1685.89844fd + 4.5898437ft - 3.58854167dt \quad (5)$$

$$R_a = 2.374347 - 0.003339v + 16.07332f - 5.205469d - 0.02125t + 0.000000231481v^2 + 14.40972222f^2 + 3.430555556d^2 + 0.00128472t^2 - 0.01212963vf + 0.00277778vd + 0.00000694444vt - 14.4140625fd + 0.15625ft + 0.023958333dt \quad (6)$$

$$W = -0.175056 + 0.000352v - 0.073322f + 0.336076d + 0.0041901t - 0.0000000720165v^2 + 0.245225694f^2 - 0.12430556d^2 + 0.00012153t^2 - 0.0000405093vf - 0.00013148vd + 0.00000347222vt + 0.16796875fd + 0.0003906ft + 0.000989583dt \quad (7)$$

where, v in m/min; f in mm/rev; d in mm; t in min; F_m in N, R_a in microns; W in mm.

The adequacy of the developed models has been tested through analysis of variance (ANOVA) method [56]. The ANOVA table consists of sum of squares and degrees of freedom. The sum of squares is performed into contributions from the polynomial model and the experimental error. The mean square is the ratio of sum of squares to degrees of freedom and F-ratio is the ratio of mean square of regression model to the mean square of the experimental error. As per ANOVA, the calculated value of F-ratio of proposed model should be more than F-table for the model to be adequate for a given confidence interval. Table 4 presents the summary ANOVA and it is found that the developed models are significant at 99% confidence interval as F-ratio of all the five models is greater than 3.13 (F-table $_{(14,\ 93,\ 0.01)}$). The goodness of fit of the proposed models was also tested through the coefficient of determination (R^2), which is the proportion of variation in the dependent parameter explained by the polynomial model. Table 4 gives the R^2 values of the proposed models, which also indicate very high correlation between the experimental and the predicted values of machinability characteristics.

The Eqs. (5) to (7) are used to test the accuracy of the developed RSM based models. The percentage prediction accuracy of the model is given by:

$$\Delta = \frac{100}{N} \sum_{i=1}^{N} \left| \frac{y_{i,\text{expt}} - y_{i,\text{pred}}}{y_{i,\text{pred}}} \right| \quad (8)$$

where, $y_{i,expt}$: measured value of response corresponding to ith trial, $y_{i,pred}$: predicted value of response corresponding to ith trial and N: number of trials. The average absolute prediction error for the experimental data of FFD was found to be 5.28%, 1.47% and 2.75% for machining force; surface roughness and tool wear models respectively.

For the validation purpose, the experiments were conducted for 36 new trials, consisting of combinations of input process parameters,

Table 4
Summary of ANOVA and R^2 values for proposed machinability models.

Machinability characteristic	Sum of squares		Degrees of freedom		Mean square		F-ratio	R^2
	Regression	Residual	Regression	Residual	Regression	Residual		
Machining force (F_m)	2982824	14391	14	93	213059	1376.89	155[a]	0.995
Surface roughness (R_a)	21.4270	0.5393	14	93	1.5305	0.0058	263.93[a]	0.975
Tool wear (W)	0.0774642	0.0015235	14	93	0.0055332	0.0000164	337.77[a]	0.981

[a] Significant at 99% confidence interval.

which do not belong to the FFD experimental data set. Table 5 presents the experimental and the predicted values of RSM based machinability models, which clearly show that the experimental and the predicted values closely agree with each other. The average absolute prediction error for the validation data was found to be around 8.10%, 3.62% and 4% for machining force, surface roughness and tool wear models respectively.

5. Results and discussion

The proposed machinability models (Eqs. (5)–(7)) are used to predict the machining force (F_m), surface roughness (R_a) and tool wear (W) by substituting the values of cutting speed (v), feed rate (f), depth of cut (d) and machining time (t) within the ranges of the process parameters selected. The two-factor interaction effects due to cutting speed (v) — feed rate (f), cutting speed (v) — depth of cut (d), cutting speed (v) — machining time (t), feed rate (f) — depth of cut (d), feed rate (f) — machining time (t) and depth of cut (d) — machining time (t) on three machinability aspects, namely, machining force (F_m), surface roughness (R_a) and tool wear (W) during hard turning of AISI 4340 high strength low alloy steel were analyzed (Figs. 2–7). These plots were generated considering two parameters at a time, while the other parameters were kept at the center level.

5.1. Analysis of machining force

Fig. 2 shows the interaction effects of cutting speed (v) — feed rate (f), cutting speed (v) — depth of cut (d) and cutting speed (v) — machining time (t) on machining force (F_m). As seen from Fig. 2, for a given value of feed rate, the machining force linearly decreases with the increase in speed and with further increase in feed rate the force increases. The probable reason might be, with the increase in cutting speed, the shear angle increases, resulting in shorter plane area/reduction in chip thickness and hence the machining force decreases. Further, with the increased feed rate, the contact area between the cutting tool and workpiece increases and hence machining force increases. It is also seen from this figure that the machining force is sensitive to feed rate variations for all values of cutting speed specified. A similar behavior is observed on machining force due to the interaction effect of cutting speed and depth of cut. On the other hand, the variation of machining force with cutting speed at different values of machining time is also found to be similar but exhibits slightly non-linear behavior. It is evident from Fig. 2 that the combination of low feed rate, low depth of cut and low machining time with high cutting speed is necessary for minimizing the machining force.

The variations due to feed rate (f) — depth of cut (d), feed rate (f) — machining time (t) and depth of cut (d) — machining time (t) on machining force (F_m) are illustrated in Fig. 3. The machining force increases non-linearly with feed rate for a given value of depth of cut and with further increase in depth of cut the machining force also increases. It is observed that the combination of low feed rate with low depth of cut is beneficial in minimizing the force. It is obvious that, at slower feed rate there is a small resistance to cutting tool in the direction of feed rate; however at larger feed rate, the work material offers more resistance to tool in the cutting direction and hence friction increases, which in turn increases the machining force. With the further increase in depth of cut, the material removal rate (MRR) increases,

Table 5
Validation data set.

Trial no.	Actual setting values of input parameters				Machinability characteristics					
					Experimental			Predicted		
	v (m/min)	f (mm/rev)	d (mm)	t (min)	F_m (N)	R_a (μm)	W (mm)	F_m (N)	R_a (μm)	W (mm)
1	115	0.15	0.95	2	678	0.93	0.089	667.38	0.98	0.0868
2	115	0.15	0.95	4	682	0.95	0.099	683.81	1.04	0.0994
3	115	0.15	0.95	6	689	0.98	0.122	703.03	1.12	0.1130
4	115	0.15	1.125	2	790	1.12	0.092	745.77	1.00	0.1026
5	115	0.15	1.125	4	795	1.14	0.104	760.95	1.07	0.1156
6	115	0.15	1.125	6	802	1.19	0.125	778.92	1.16	0.1295
7	115	0.23	0.95	2	845	1.26	0.095	820.12	1.52	0.1008
8	115	0.23	0.95	4	848	1.28	0.116	837.29	1.61	0.1135
9	115	0.23	0.95	6	852	1.32	0.129	857.24	1.71	0.1272
10	115	0.23	1.125	2	895	1.45	0.099	922.12	1.34	0.1190
11	115	0.23	1.125	4	902	1.48	0.118	938.03	1.44	0.1320
12	115	0.23	1.125	6	908	1.54	0.132	956.73	1.55	0.1460
13	175	0.15	0.95	2	645	0.88	0.097	629.80	0.83	0.0993
14	175	0.15	0.95	4	648	0.91	0.110	645.86	0.90	0.1123
15	175	0.15	0.95	6	655	0.94	0.127	664.70	0.98	0.1263
16	175	0.15	1.125	2	728	0.92	0.108	710.93	0.88	0.1137
17	175	0.15	1.125	4	730	0.94	0.126	725.73	0.96	0.1271
18	175	0.15	1.125	6	735	0.96	0.1443	743.32	1.04	0.1415
19	175	0.23	0.95	2	810	1.18	0.112	782.09	1.31	0.1131
20	175	0.23	0.95	4	814	1.19	0.128	798.88	1.41	0.1262
21	175	0.23	0.95	6	818	1.22	0.148	818.46	1.51	0.1403
22	175	0.23	1.125	2	833	1.29	0.122	886.81	1.16	0.1299
23	175	0.23	1.125	4	838	1.32	0.141	902.35	1.26	0.1434
24	175	0.23	1.125	6	842	1.35	0.158	920.67	1.37	0.1578
25	235	0.15	0.95	2	615	0.72	0.114	597.34	0.69	0.1112
26	235	0.15	0.95	4	619	0.74	0.125	613.01	0.75	0.1247
27	235	0.15	0.95	6	624	0.77	0.136	631.48	0.83	0.1392
28	235	0.15	1.125	2	756	0.81	0.119	681.19	0.76	0.1243
29	235	0.15	1.125	4	759	0.83	0.144	695.61	0.84	0.1381
30	235	0.15	1.125	6	765	0.83	0.158	712.82	0.93	0.1529
31	235	0.23	0.95	2	775	1.05	0.132	749.16	1.11	0.1249
32	235	0.23	0.95	4	778	1.08	0.146	765.57	1.20	0.1384
33	235	0.23	0.95	6	784	1.12	0.154	784.77	1.31	0.1529
34	235	0.23	1.125	2	803	1.11	0.135	856.61	0.99	0.1403
35	235	0.23	1.125	4	805	1.13	0.152	871.77	1.09	0.1542
36	235	0.23	1.125	6	810	1.15	0.168	889.71	1.20	0.1691

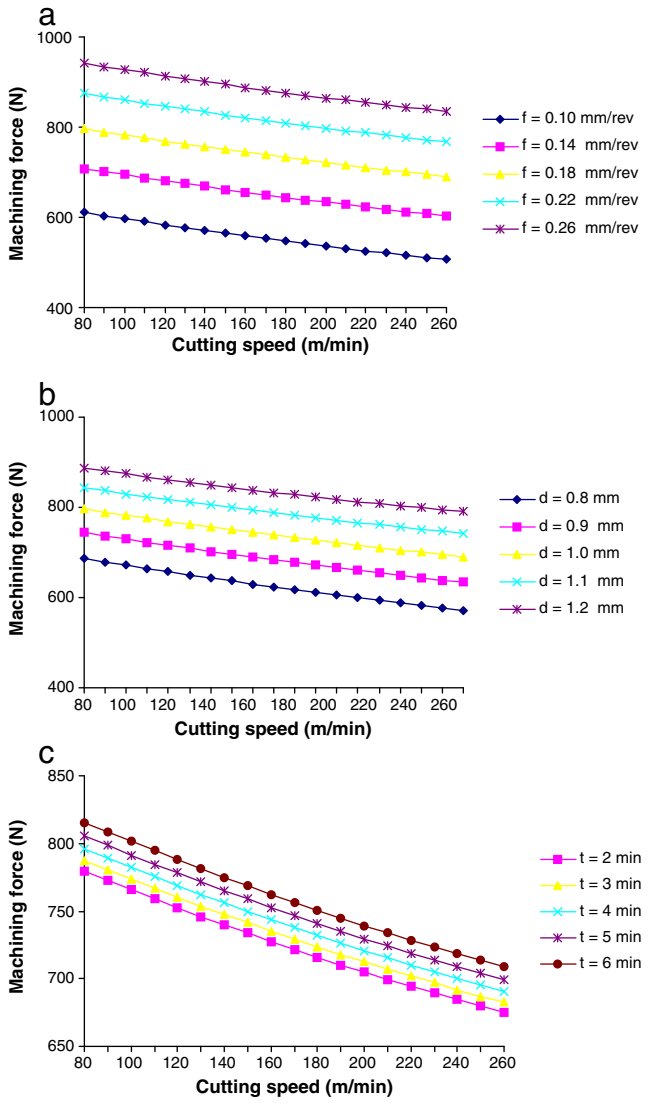

Fig. 2. Effect of (a) cutting speed and feed rate (b) cutting speed and depth of cut (c) cutting speed and machining time on machining force.

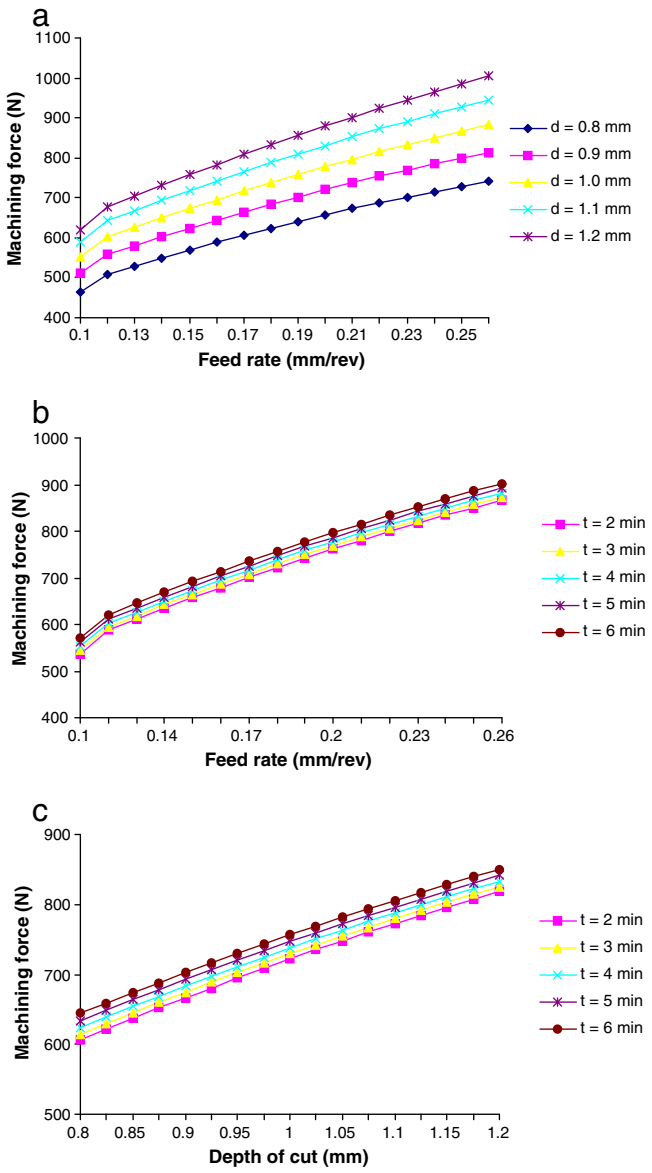

Fig. 3. Effect of (a) feed rate and depth of cut (b) feed rate and machining time (c) depth of cut and machining time on machining force.

which contribute to increase in machining force. As shown in Fig. 3, the variations due to feed rate–machining time and depth of cut–machining time on the machining force are almost showing similar behavior as that of feed rate–depth of cut interaction. But both the interactions have negligible effects on machining force. Fig. 3 clearly suggests that the machining force can be minimized by employing lower values of feed rate, depth of cut and machining time with higher cutting speed.

5.2. Analysis of surface roughness

Fig. 4 depicts the estimated surface roughness in relation to cutting speed (v)–feed rate (f), cutting speed (v)–depth of cut (d) and cutting speed (v)–machining time (t) interactions on surface roughness (R_a). It is seen that all the above interactions demonstrate linear variations on surface roughness and the behavior is more or less same. The surface roughness decreases sharply with increase in cutting speed for a given value of feed rate and with further increase in feed rate the machining force increases. This is due to the fact that, as cutting speed increases, the temperature increases at the cutting zone that leads to the softening of material and thus reduces the surface roughness. With increased feed rate, thrust force increases, leading to vibration and generating more heat and thereby resulting higher surface roughness. It is observed from Fig. 4 that surface roughness is sensitive to variations in feed rate at lower values of cutting speed as compared to higher cutting speed values. The surface roughness is found to be minimal at high cutting speed with low feed rate. On the other hand, similar behavior is observed for surface roughness due to the interaction effect of cutting speed–machining time. But the surface roughness is insensitive to variations in machining time irrespective of the cutting speed specified. It is also revealed that a combination of higher cutting speed along with lower machining time is necessary for minimizing the surface roughness. It is seen form Fig. 4 that the surface roughness is minimal for higher cutting speed (260 m/min) with medium depth of cut (1 mm), which shows that an effective material removal has been taken place. On the other hand, effective material removal might not have taken place at lower depth of cut, mainly due to predominant rubbing and ploughing action and hence higher surface roughness. Fig. 4 also indicates that surface roughness is highly sensitive to variations in depth cut at lower values of cutting speed as compared to higher cutting speed values.

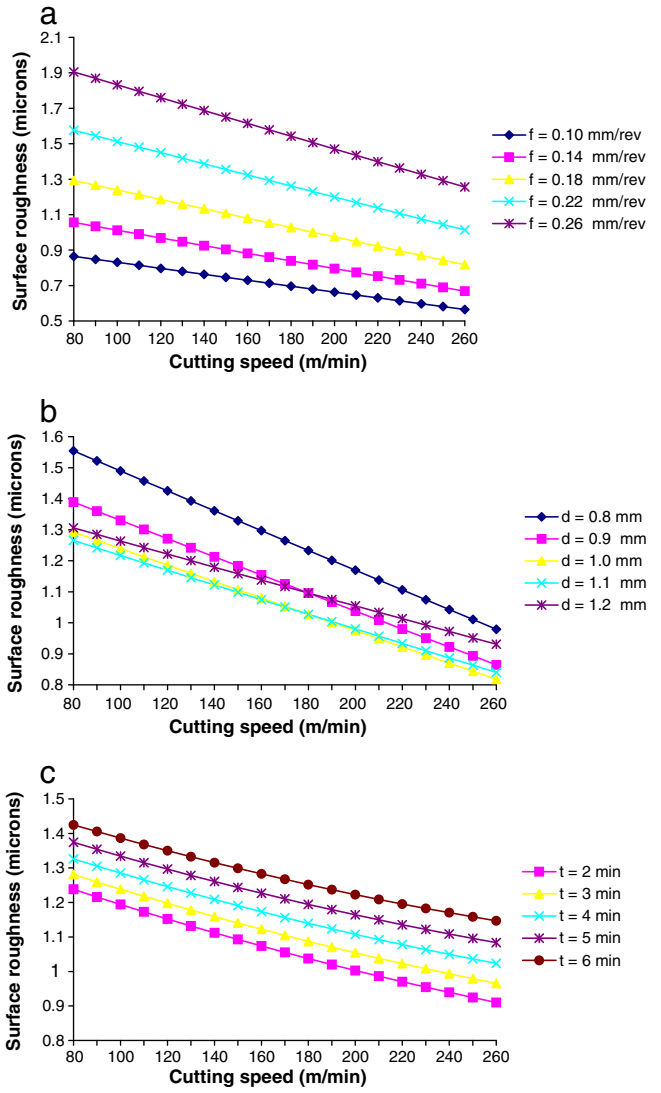

Fig. 4. Effect of (a) cutting speed and feed rate (b) cutting speed and depth of cut (c) cutting speed and machining time on surface roughness.

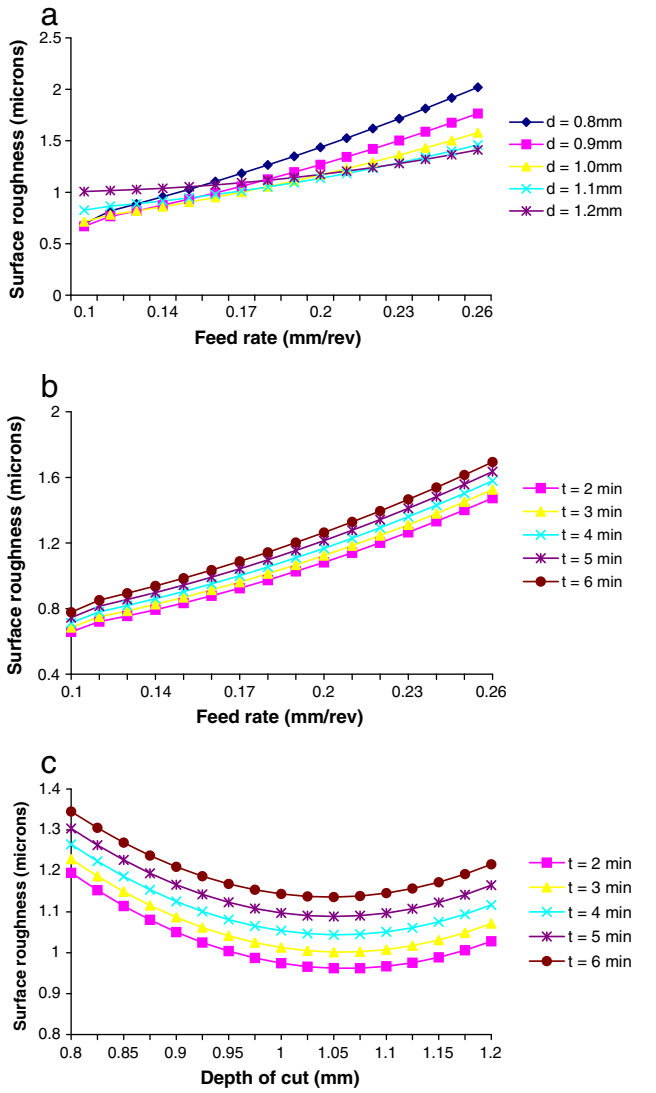

Fig. 5. Effect of (a) feed rate and depth of cut (b) feed rate and machining time (c) depth of cut and machining time on surface roughness.

The graphs showing the interaction effects of feed rate (f)–depth of cut (d), feed rate (f)–machining time (t) and depth of cut (d)–machining time (t) on surface roughness (R_a) are presented in Fig. 5. As seen from this figure, surface roughness increases with feed rate for a given value of depth of cut and roughness is found to be sensitive to variations in depth of cut at higher values of feed rate as compared to lower values. The reduced surface roughness is observed at a combination of lower feed rate (0.1 mm/rev) and medium depth of cut (1 mm). On the other hand, surface roughness increases with increase in feed rate for a given value of machining time and the surface roughness increases further with prolonged machining time. However, surface roughness is insensitive to variations in machining time irrespective of the feed rate. Fig. 5 also indicates that there exists synergistic interaction due to depth of cut and machining time on surface roughness. For a specified value of machining time, the surface roughness initially decreases non-linearly with increase in depth of cut up to 1 mm and then increases. With prolonged machining time the surface roughness further increases. Fig. 6 shows the scanning electron microscopy (SEM) images in the quality of the surface observed during turning of AISI 4340 high strength low alloy steel using coated carbide tool for two different depth of cuts (0.8 mm and 1 mm) for a higher cutting speed of 260 m/min, feed rate of 0.1 mm/rev and a machining time of 4 min. The improved surface finish is clearly evidenced in Fig. 6 for reduced depth of cut.

5.3. Analysis of tool wear

Fig. 7 shows the behavior of tool wear (W) in relation to cutting speed (v)–feed rate (f), cutting speed (v)–depth of cut (d) and cutting speed (v)–machining time (t) interactions. As seen from this figure, tool wear linearly increases with increase in cutting speed for all values of feed rates selected in the range 0.1–0.26 mm and sensitive to feed rate variations for all values of cutting speed specified. On the other hand, both cutting speed–depth of cut and cutting speed–machining time interactions also demonstrate similar behavior on tool wear. The increase in tool wear at higher values of cutting speed is probably due to the abrasion at the rake face of the tool as the machining time progresses. It is also observed from Fig. 7 that the tool wear is sensitive to variations in depth of cut at lower values of cutting speed as compared to higher values.

The effects of feed rate–depth of cut, feed rate–machining time and depth of cut–machining time on tool wear are displayed in Fig. 8, which clearly demonstrate similar behavior. Hence, from Figs. 7 and 8, it is clear that a combination of lower values of cutting

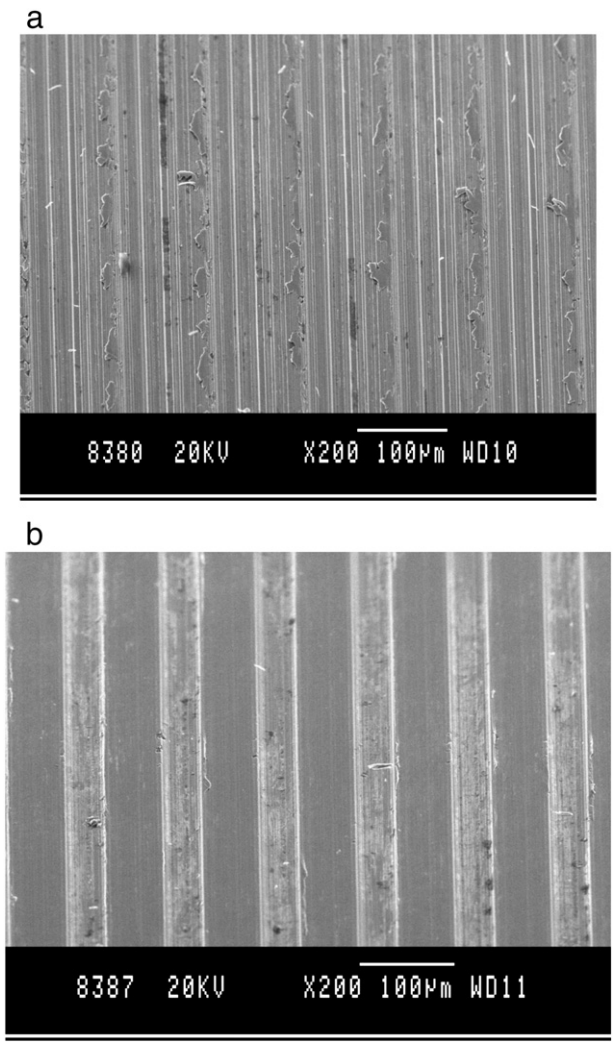

Fig. 6. SEM images of the surface quality observed during turning of AISI 4340 high strength low alloy steel: (a) v = 260 m/min, f = 0.1 mm/rev, t = 4 min and d = 0.8 mm; and (b) v = 260 m/min, f = 0.1 mm/rev, t = 4 min and d = 1 mm.

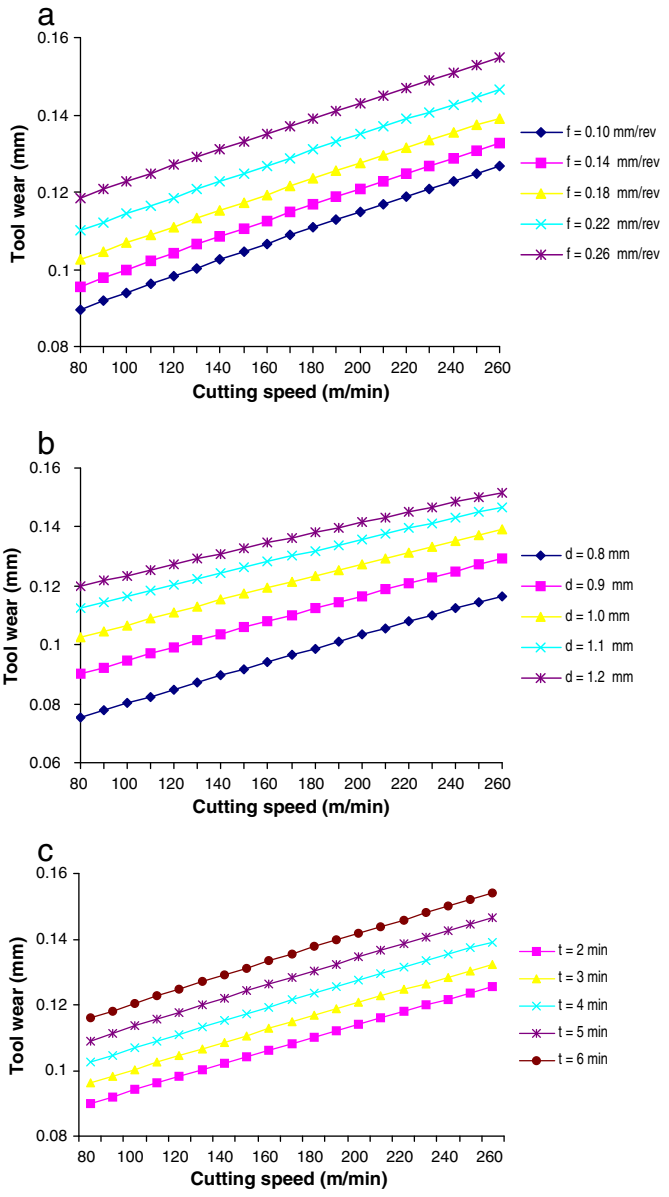

Fig. 7. Effect of (a) cutting speed and feed rate (b) cutting speed and depth of cut (c) cutting speed and machining time on tool wear.

speed, feed rate, depth of cut and machining time is beneficial in reducing the tool wear. The reason might be at higher values of feed rate and depth of cut, contact between cutting tool and workpiece increases and hence higher tool wear. Fig. 9 shows the wear of the coated carbide-cutting tool observed with the scanning electron microscopy (SEM) after the machining tests. The formation of the wear is due to the occurrence of higher pressure and temperature at the tool. Fig. 9(a) gives the grooves observed on the rake face tool wear for cutting speed of 200 m/min, feed rate of 0.1 mm/rev, machining time of 2 min and 1 mm depth of cut. The reason for the occurrence of the grooves is due to the abrasive mechanism and adhesion of the material. It is also revealed from the investigation that the tool wear is concentrated typically on the nose region because of higher stresses and thermal softening of tool material due to higher temperature at this region. The chipping of the tool cutting edge is seen in Fig. 9(b) for cutting speed of 260 m/min, feed rate of 0.26 mm/rev and 1.2 mm depth of cut, which indicates the prominent tool wear at higher values of cutting conditions.

5.4. Chip analysis

The knowledge of chip forming process is necessary to understand the condition of the newly formed surface in turning and hence an attempt has also been made in the current investigation to study the chip morphology in addition to the machinability aspects. In general, at lower cutting conditions short broken irregular shaped chips were obtained. The probable reason may be at low cutting conditions rubbing and abrasive actions are more predominant than the actual machining and hence irregular shaped chips are produced. With increased feed rate loose arc chips, with increased speed continuous chips and with increased depth of cut long continuous chips were observed. The continuous chips at above conditions are probably due to effective machining because of shearing of workpiece leading to plastic deformation. The chip breaking was also seen at higher cutting speeds. On the other hand, curled chips were seen at high cutting speed with lower feed rate and depth of cut. Fig. 10 presents some aspects of chips obtained in the present investigation under various cutting conditions during turning of AISI 4340 high strength low alloy steel using coated carbide tool. In all the cases, medium feed rate of 0.18 mm/rev was kept constant. At low cutting speed and low depth of cut, long loose arc type thin chips were produced (Fig. 10a). When cutting speed is increased from low to high, shorter loose arc chips with up and side curling were observed (Fig. 10b). On the

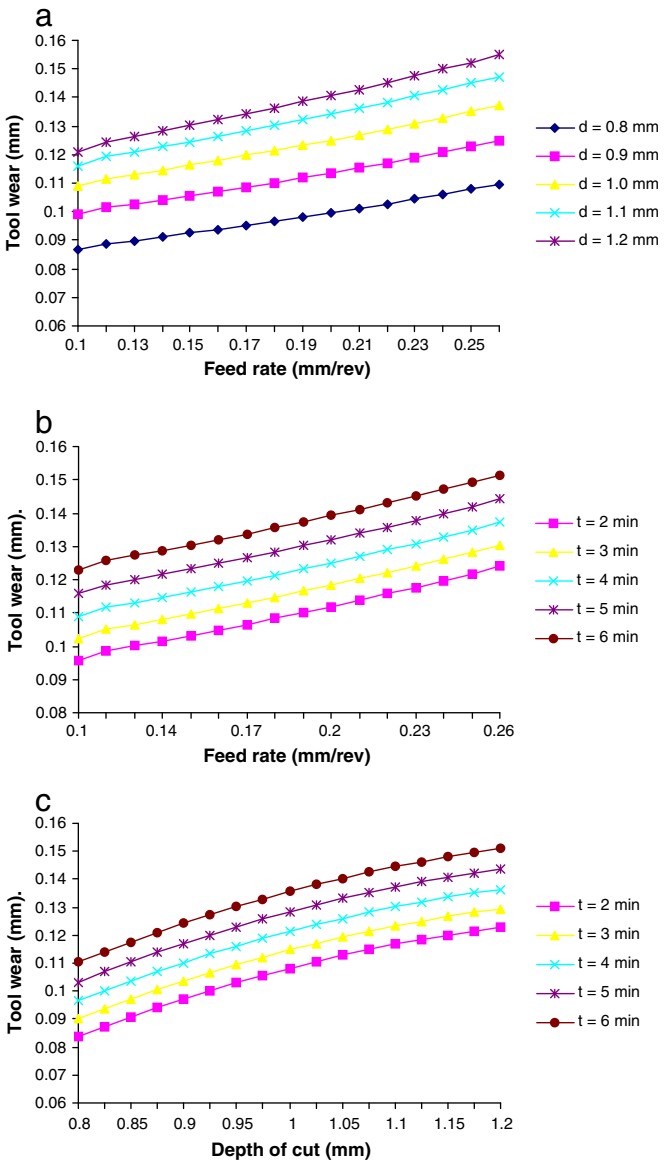

Fig. 8. Effect of (a) feed rate and depth of cut (b) feed rate and machining time (c) depth of cut and machining time on tool wear.

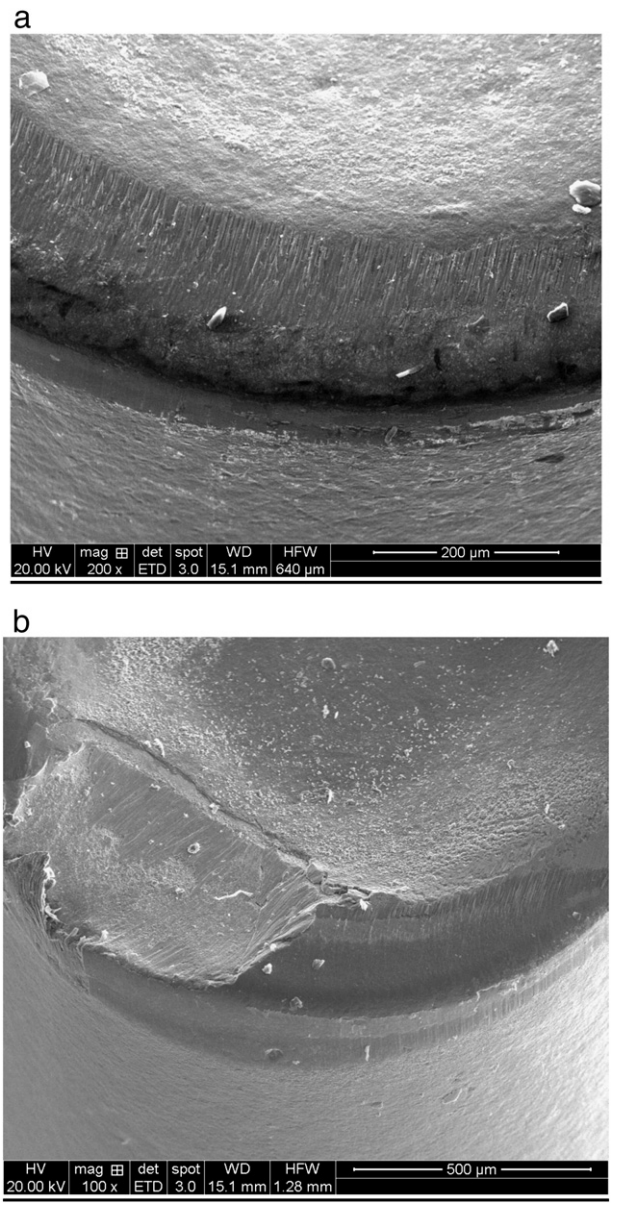

Fig. 9. SEM images of the wear of cutting tool: (a) v = 200 m/min, f = 0.1 mm/rev, t = 2 min and d = 1 mm; and (b) v = 260 m/min, f = 0.26 mm/rev, t = 2 min and d = 1.2 mm.

other hand, when cutting speed is increased from low to medium and depth of cut from low to high, long continuous tubular structured coiled type chips were obtained (Fig. 10c). At higher cutting speed with higher depth of cut short saw toothed loose arc thick chips were produced (Fig. 10d).

6. Conclusions

In the present investigation, the various machinability aspects such as machining force, surface roughness and tool wear were analyzed to study the effects of cutting speed, feed rate, depth of cut and machining time in hard turning of AISI 4340 high strength low alloy steel using coated carbide insert. The experiments were planned as per full factorial design and the response surface methodology has been employed for the machinability study. Analysis of variance has been carried out to check the adequacy of the proposed machinability models. Based on the experimental results and the subsequent parametric analysis the following conclusions are drawn within the ranges of the process parameters selected:

- For a given value of feed rate, the machining force decreases with increase in speed and with further increase in feed rate the force increases. The machining force is sensitive to feed rate variations for all values of cutting speed specified. A similar behavior is observed due to interaction effects of cutting speed–depth of cut and cutting speed–machining time on machining force.
- The machining force increases with feed rate for a given value of depth of cut and with further increase in depth of cut the machining force also increases.
- The combination of low feed rate, low depth of cut and low machining time with high cutting speed is beneficial for minimizing the machining force.
- The surface roughness is sensitive to variations in feed rate at lower values of cutting speed as compared to higher cutting speed values. The surface roughness is highly sensitive to variations in depth cut at lower values of cutting speed as compared to higher cutting speed values. But the surface roughness is found to be insensitive to variations in machining time irrespective of the cutting speed specified.

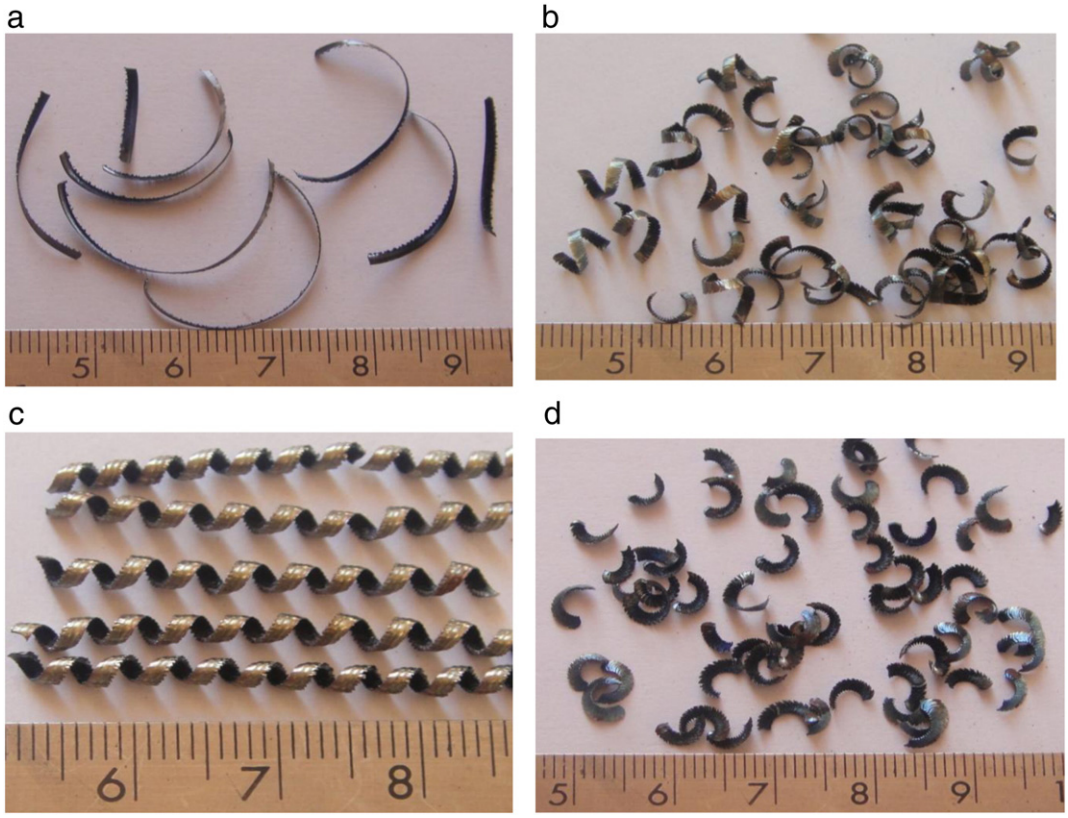

Fig. 10. Aspects of chips obtained as function of cutting conditions (30×magnification): (a) At cutting conditions v = 140 m/min, f = 0.18 mm/rev and d = 0.8 mm (b) At cutting conditions v = 260 m/min, f = 0.18 mm/rev and d = 0.8 mm (c) At cutting conditions v = 200 m/min, f = 0.18 mm/rev and d = 1.2 mm (d) At cutting conditions v = 260 m/min, f = 0.18 mm/rev and d = 1.2 mm.

- Better surface quality is observed at higher cutting speed with lower feed rate.
- The cutting tool wear increases with increase in cutting speed for all values of feed rates and sensitive to feed rate variations for all values of cutting speed specified. Tool wear is also sensitive to variations in depth of cut at lower values of cutting speed as compared to higher values.
- Tool wear can be minimized by employing lower values of cutting speed, feed rate, depth of cut and machining time.
- Based on the operating cutting conditions, various chips such as short broken irregular shaped, loose arc, continuous, long continuous tubular structured coiled and short saw toothed loose arc thick types are formed.
- The chip breaking is observed at high cutting speeds.

References

[1] Zou JM, Anderson M, Stahl JE. Identification of cutting errors in precision hard turning process. J Mater Process Technol 2004;153–154:746–50.
[2] Rech J, Moisan A. Surface integrity in finish hard turning of case hardened steels. Int J Mach Tool Manuf 2003;43:543–50.
[3] Destefani J. Technology key to mold making success. Manuf Eng 2004;133(4):59–64.
[4] Elbestawi MA, Chen L, Becze CE, El-Wardany TI. High-speed milling of dies and molds in their hardened state. Ann CIRP 1997;46(1):57–62.
[5] Tonshoff HK, Wobker HG, Brandt D. Hard turning — influence on the workpiece properties. Trans NAMRI/SME 1995;23:215–20.
[6] Fnides B, Yallese MA, Aouici H. Hard turning of hot work steel AISI H11: evaluation of cutting pressures, resulting force and temperature. Mech Kaunas Technol Nr 2008;4(72):59–63.
[7] Fnides B, Yallese MA, Mabrouki T. Surface roughness model in turning hardened hot work steel using mixed ceramic tool. Mech Kaunas Technol Nr 2009;3(77):68–73.
[8] Bouacha K, Yallese MA, Mabrouki T. Statistical analysis of surface roughness and cutting forces using response surface methodology in hard turning of AISI 52100 bearing steel with CBN tool. Int J Refract Met Hard Mater 2010;28:349–61.
[9] Byrne G, Dornfeld D, Denkena B. Advancing cutting technology. Ann CIRP 2003;52(2):483–507.
[10] Klocke F, Brinskmeier E, Weinert K. Capability profile of hard cutting and grinding processes. Ann CIRP 2005;54(2):557–80.
[11] Guo YB. Sahni JA comparative study of hard turned and cylindrically ground white layers. Int J Mach Tool Manuf 2004;44:135–45.
[12] Huang Y, Liang SY. Cutting forces modeling considering the effect of tool thermal property — application to CBN hard turning. Int J Mach Tool Manuf 2003;43:307–15.
[13] Thiele JD, Melkote SN, Peascoe RA, Watkins TR. Effect of cutting edge geometry and workpiece hardness on surface residual stresses in finish hard turning of AISI 52100 steel. ASME J Manuf Sci Eng 2000;122:642–9.
[14] Sahin Y, Motorcu AR. Surface roughness model for machining mild steel with coated carbide tool. Mater Des 2005;26(4):321–6.
[15] Lima JG, Avila RF, Abrao AM, Faustino M, Davim JP. Hard turning AISI 4340 high strength low alloy steel and AISI D2 cold work steel. J Mater Process Technol 2005;169:388–95.
[16] Luo SY, Liao YS, Tsai YY. Wear characteristics in turning high hardness alloy steel by ceramic and CBN tools. J Mater Process Technol 1995;88:114–21.
[17] Yallase MA, Chaoui K, Zeghib M, Boulanouar L, Rigal JF. Hard machining of hardened bearing steel using cubic boron nitride tool. J Mater Process Technol 2009;209:1092–104.
[18] Davim JP, Figueira L. Machinability evaluation in hard turning of cold work tool steel (D2) with ceramic tools using statistical techniques. Mater Des 2007;28:1186–91.
[19] Ozel T, Karpat Y. Predictive modeling of surface roughness and tool wear in hard turning using regression and neural networks. Int J Mach Tool Manuf 2005;4:467–79.
[20] Quiza R, Figueira L, Davim JP. Comparing statistical models and artificial networks on predicting the tool wear in hard machining D2 AISI steel. Int J Adv Manuf Technol 2008;37:641–8.
[21] Tamizharasan T, Selvaraj T, Haq AN. Analysis of tool wear and surface finish in hard turning. Int J Adv Manuf Technol 2006;28:671–9.
[22] Oliveira AJ, Diniz AE, Ursolino DJ. Hard turning in continuous and interrupted cut with PCBN and whisker reinforced cutting tools. J Mater Process Technol 2009;209:5262–70.
[23] Jiang W, More AS, Brown WD, Malshe AP. A CBN–TiN composite coating for carbide inserts: coating characterization and its application for finish hard turning. Surf Coat Technol 2006;201:2443–9.
[24] Aslan E. Experimental investigation of cutting tool performance in high speed cutting of hardened X210Cr12 cold-work tool steel (62 HRC). Mater Des 2005;26:21–7.

[25] Yigit R, Celik E, Findik F, Koksal S. Tool life performance of multilayer hard coatings produced by HTCVD for machining of nodular cast iron. Int J Refract Met Hard Mater 2008;26:514–24.
[26] Aneiro FM, Coelho RT, Brandao LC. Turning hardened steel using coated carbide at high cutting speeds. J Braz Soc Mech Sci Eng 2008;30(2):104–9.
[27] Knutsson A, Johansson MP, Karlsson L, Oden M. Machining performance and decomposition of TiAlN/TiN multilayer coated metal cutting inserts. Surf Coat Technol 2011;205:4005–10.
[28] Yigit R, Celik E, Findik F. Performance of multilayer coated carbide tools when turning cast iron. Turk J Eng Environ Sci 2009;33:147–57.
[29] Ciftci I. Machining of austenitic stainless steels using CVD multi-layer coated cemented carbide tools. Tribol Int 2006;39:565–9.
[30] Bouzakis KD, Hadjiyiannis S, Skordaris G. The Influence of the coating thickness on its strength properties and on the milling performance of PVD coated inserts. Surf Coat Technol 2003;174–175:393–401.
[31] Grzesik W. Influence of tool wear on surface roughness in hard turning using differently shaped ceramic tools. Wear 2008;265:327–35.
[32] Gaitonde VN, Karnik SR, Figueira L, Davim JP. Machinability investigations in hard turning of AISI D2 cold work tool steel with conventional and wiper ceramic inserts. Int J Refract Met Hard Mater 2009;27:754–63.
[33] Gaitonde VN, Karnik SR, Figueira L, Davim JP. Analysis of machinability during hard turning of cold work tool steel (Type: AISI D2). Mater Manuf Process 2009;24(12):1373–82.
[34] Gaitonde VN, Karnik SR, Figueira L, Davim JP. Performance comparison of conventional and wiper ceramic inserts in hard turning through artificial neural network modeling. Int J Adv Manuf Technol 2011;52(1–4):101–14.
[35] Arsecularatne JA, Zhang LC, Montross C, Mathow P. On machining of hardened AISI D2 steel with PCBN tools. J Mater Process Technol 2007;171:244–52.
[36] Kumar AS, Durai AR, Sornakumar T. The effect of tool wear on tool life of alumina-based ceramic cutting tools while machining hardened martensitic steels. J Mater Process Technol 2006;173:151–6.
[37] More AS, Jiang W, Brown WD, Malshe AP. Tool wear and machining performance of CBN–TiN coated carbide inserts and PCBN compact inserts in turning AISI 4340 hardened steel. J Mater Process Technol 2006;180:253–62.
[38] Chou YK, Evans CJ. Tool wear mechanism in continuous cutting of hardened tool steels. Wear 1997;212:59–65.
[39] Chou YK, Evans CJ, Barash MM. Experimental investigation on CBN turning of hardened AISI 52100 steel. J Mater Process Technol 2002;124:274–83.
[40] Thiele JD, Melkote SN. Effect of cutting edge geometry and workpiece hardness on surface generation in the finish hard turning of AISI 52100 steel. J Mater Process Technol 1999;94:216–26.
[41] Ozel T, Hsu T-K, Zeren E. Effects of cutting edge geometry, workpiece hardness, feed rate and cutting speed on surface roughness and forces in finish turning of hardened AISI H13 steel. Int J Adv Manuf Technol 2000;25(3–4):262–9.
[42] Poulachon G, Bandyopadhyay BP, Jawahir IS, Pheulpin S, Seguin E. The influence of the microstructure of hardened tool steel workpiece on the wear of PCBN cutting tools. Int J Mach Tool Manuf 2003;43:139–44.
[43] El-Wardany TI, Kishawy HA, Elbestawi MA. Surface integrity of die material in high-speed hard machining, Part 1, micro graphical analysis. ASME J Manuf Sci Eng 2000;122(4):620–31.
[44] El-Wardany TI, Kishawy HA, Elbestawi MA. Surface integrity of die material in high-speed hard machining, Part 2, micro hardness variations and residual stresses. ASME J Manuf Sci Eng 2000;122(4):632–41.
[45] Kishawy HA, Elbestawi MA. Tool wear and surface integrity during high-speed turning hardened steel with polycrystalline cubic boron nitride tools. J Eng Manuf 2001;215:755–67.
[46] Chou YK, Song H. Tool nose radius effects on finish turning. J Mater Process Technol 2004;148:259–68.
[47] Benga GC, Abrao AM. Turning of hardened 100Cr6 bearing steel with ceramic and PCBN cutting tools. J Mater Process Technol 2003;143–144:237–41.
[48] Kumar AS, Durai R, Sornakumar T. Machinability of hardened steel using alumina based ceramic cutting tools. Int J Refract Met Hard Mater 2003;21:109–17.
[49] Grzesik W, Wanat T. Comparative assessment of surface roughness produced by hard machining with mixed ceramic tools including 2D and 3D analysis. J Mater Process Technol 2005;169:364–71.
[50] Grzesik W, Wanat T. Hard turning of quenched alloy steel parts using conventional and wiper ceramic inserts. Int J Mach Tool Manuf 2006;46:1988–95.
[51] Klocke F, Kratz H. Advanced tool edge geometry for high precision hard turning. Ann CIRP 2005;54(1):47–50.
[52] Schwach DW, Guo YB. Feasibility of producing optimal surface integrity by process design in hard turning. Mater Sci Eng 2005;395:116–23.
[53] Pavel R, Marinescu I, Deis M, Pillar J. Effect of tool wear on surface finish for a case of continuous and interrupted hard turning. J Mater Process Technol 2005;170:341–9.
[54] Diniz AE, Oliveira AJ. Hard turning of interrupted surfaces using CBN tools. J Mater Process Technol 2008;195:275–81.
[55] Ezugwu EO, Silva RB, Bonney JA, Machado R. Evaluation of the performance of CBN when turning Ti-6Al-4V alloy with high pressure coolant supplies. Int J Mach Tool Manuf 2005;45(9):1009–14.
[56] Montgomery DC. Design and analysis of experiments. New York: John Wiley; 2004.